



## Review

## Measurements of extremely low radioactivity levels in stainless steel for GERDA

W. Maneschg<sup>a,\*</sup>, M. Laubenstein<sup>b</sup>, D. Budjáč<sup>a</sup>, W. Hampel<sup>a</sup>, G. Heusser<sup>a</sup>, K.T. Knöpfle<sup>a</sup>,  
B. Schwingenheuer<sup>a</sup>, H. Simgen<sup>a</sup>

<sup>a</sup> Max-Planck-Institut für Kernphysik, Saupfercheckweg 1, D-69117 Heidelberg, Germany

<sup>b</sup> Laboratori Nazionali del Gran Sasso (LNGS), S.S. 17 km/bis km 18+910, I-67010 Assergi (AQ), Italy

## ARTICLE INFO

## Article history:

Received 30 March 2008

Received in revised form

23 May 2008

Accepted 25 May 2008

Available online 18 June 2008

## Keywords:

Double beta decay

Low-radioactivity

Gamma spectroscopy

Stainless steel

## ABSTRACT

The radioisotope concentrations in stainless steel for the cryostat of the GERDA experiment at the Laboratori Nazionali del Gran Sasso (LNGS) have been measured. A total of 13 different stainless steel batches have been screened by low-level  $\gamma$ -ray spectrometry with germanium detectors located at two underground laboratories. The article reports the discovery of commonly available stainless steel with very low concentrations of primordial and cosmogenic radionuclides. The concentrations are in the range of 1 mBq/kg and below. Only the manmade <sup>60</sup>Co-isotope is present in all samples with a higher concentration of around 19 mBq/kg. Further, deviations from secular equilibrium in the natural decay chains of U and Th have been observed in some cases.

© 2008 Elsevier B.V. All rights reserved.

## Contents

1. Introduction	448
2. Measurement of radioactivity in stainless steel	449
2.1. Selection of stainless steel samples and preparation	449
2.2. Screening techniques and measurement procedure	449
3. Process of evaluation	450
3.1. Efficiency determination via Monte Carlo simulations	450
3.2. Calculation of the radioactivity concentrations	450
4. Discussion of the results	450
4.1. Primordial radionuclides	450
4.1.1. Representativeness of the measurements	451
4.1.2. Deviations from secular equilibrium in the <sup>238</sup> U and <sup>232</sup> Th decay chains	451
4.2. Anthropogenic radionuclides	452
4.2.1. <sup>60</sup> Co	452
4.2.2. <sup>137</sup> Cs	452
4.3. Cosmogenic radionuclides	452
4.3.1. <sup>7</sup> Be	452
4.3.2. Others	452
5. Conclusions	452
Acknowledgments	453
References	453

### 1. Introduction

The GERmanium Detector Array (GERDA experiment) is a new double beta decay experiment at the INFN Gran Sasso National

\* Corresponding author. Tel.: +49 6221 516 530; fax: +49 6221 516 802.

E-mail address: [werner.maneschg@mpi-hd.mpg.de](mailto:werner.maneschg@mpi-hd.mpg.de) (W. Maneschg).

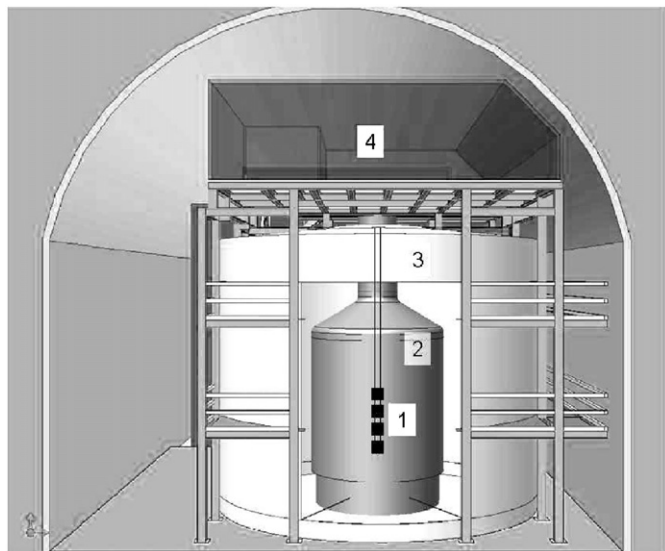


**Fig. 1.** Cross-section of the GERDA experiment in Hall A at LNGS: 1.  $^{76}\text{Ge}$ -Diode-Array. 2. Cryostat (filled with LAr). 3. Water-detector (passive shielding and muon veto). 4. Clean room with lock-system.

Laboratory (LNGS) in Italy, which will use germanium, enriched in  $^{76}\text{Ge}$ , as source and detector [1].

To reach the intended background index of  $10^{-3}$  cts/(keVkg y) in the region of 2039 keV [2] (the  $Q_{\beta\beta}$ -value of the neutrinoless  $^{76}\text{Ge}$  decay), an effective background suppression is required. The design of the experiment involves a  $65\text{ m}^3$  cryostat placed at the center of a water tank. The cryostat is filled with Liquid Argon (LAr), in which the bare Ge-diodes are operated (see Fig. 1). The LAr serves as cooling medium for the diodes and as passive shield against  $\gamma$ -quanta from surrounding materials. Its scintillation property is under investigation as an additional background discrimination technique.

The cryostat itself must be made of low-activity materials. Especially the high energetic  $^{208}\text{Tl}$ -line ( $^{228}\text{Th}$ ) at 2615 keV is critical. For economical reasons, a superinsulated two-vessel tank made of stainless steel and an inner shielding made of very pure copper<sup>1</sup> was chosen.

The amount of costly copper in the mentioned configuration depends drastically on the residual contamination in the used stainless steel: simulations for GERDA showed that a contamination of 10, 3, 1 mBq/kg  $^{228}\text{Th}$  would require 41, 23, 8 tons of copper, respectively [4]. Thus, the search for pure batches of stainless steel is important. In previous experiments, stainless steel with  $^{228}\text{Th}$ -concentrations of (5–12) mBq/kg has been identified [5]. Our goal was to find batches with similar levels in contamination around 10 mBq/kg  $^{228}\text{Th}$  or less using highly sensitive  $\gamma$ -ray spectrometry.

## 2. Measurement of radioactivity in stainless steel

### 2.1. Selection of stainless steel samples and preparation

The search for stainless steel batches focused on the austenitic 1.4571 material (DIN EN 10088 [6]). Because of its content of molybdenum (see Table 1), this stainless steel type allows high corrosion resistance. Further, it is quite common on the German market, so that the German stainless steel trading company

**Table 1**

Chemical composition of 1.4571 stainless steel; the main alloy components are given in percentage [%], the rest consists of Fe [6]

Standard: DIN EN 10088									
Material: X6CrNiMoTi17-12-2									
Material number: 1.4571									
Element	C	Si	Mn	P	S	Cr	Mo	Ni	Ti
Min						16.50	2.00	10.50	(5 × C)
Max	≤0.08	≤1.00	≤2.00	≤0.045	≤0.015	18.50	2.50	13.50	0.70

Nironit agreed to cooperate with the Max-Planck-Institut für Kernphysik (MPI-K), which is responsible for the GERDA cryostat, i.e. steel, which was too radioactive, could be returned.

Thus, stainless steel samples belonging to ton-scale batches from different European manufacturers (see Section 4) have been acquired from Nironit and are taken for material screening. Each sample consisted of a varying number of plates fitting into the sample chambers of the used germanium detectors (see Fig. 2). The total weight of a sample was in the range of (40–61) kg.

All samples underwent the same cleaning procedure at the MPI-K before starting with the measurements. The steps of this chemical procedure, which took approx. 1.5 h/sample, were as follows:

- cleaning with acetone;
- degreasing in a biological bath at 80 °C: decomposition of the incorporated oil by microorganisms; (Bio-Circle™L);
- rinsing with tap water and deionized water;
- basic solution in combination with an ultrasonic bath at 80 °C: the solution contained 5% highly concentrated grease-solving base (ph-value: 12.9) (*Tickopur R 33*);
- rinsing with deionized water;
- ultrasonic bath with deionized water: removal of the base residue;
- drying in furnace at 100 °C: the samples stayed there until the moment of extraction/package.

### 2.2. Screening techniques and measurement procedure

The measurements were carried out in the underground laboratories at MPI-K in Heidelberg (Germany) and at LNGS in Assergi (Italy). In both cases, germanium  $\gamma$ -ray spectrometers especially suited for large samples, named DARIO [7] and GeMPI [3,8], were used. Their main characteristics are listed in Table 2.

To achieve high sensitivities, these germanium detectors use different background suppression techniques and have relatively large sample chambers. DARIO is located at a shallow depth (15 m w.e.) and uses an active veto reducing the muon induced background by a factor of 13 [9]. Unlike Dario, GeMPI does not need an active veto because of the reduced muon flux at LNGS (approx.  $10^6$  times weaker than on the surface at sea level) due to the rock overburden of about 3500 m w.e. Furthermore, the complete cryostat systems of the detectors and their shieldings were made of specially selected low activity materials. Finally, the airborne contamination, which is dominated by  $^{222}\text{Rn}$  (followed by the decay of the daughters  $^{214}\text{Pb}$  and  $^{214}\text{Bi}$ ) and which can diffuse through the standard shielding, has to be suppressed. In the case of DARIO this is achieved by first pumping and subsequent flushing of the sample chamber with nitrogen gas once a week. GeMPI has an airlock system combined with an airtight steel casing around the shield, which is flushed continuously with boil-off nitrogen at slight overpressure. To minimize the residual surface contamination from  $^{222}\text{Rn}$

<sup>1</sup> Concentrations with an upper limit of  $<19\text{ }\mu\text{Bq/kg}$   $^{228}\text{Th}$  for electrolytically produced copper are reported in Ref. [3].

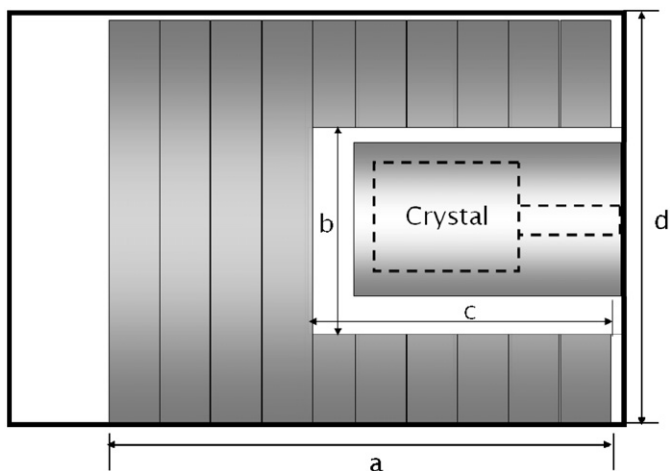


**Fig. 2.** Schematic cross-section of DARIO's sample chamber ( $20 \times 20 \times 27$ ) cm<sup>3</sup> filled with a stainless steel sample: plates (edge length  $d = 19.8$  cm) with a hole (diameter  $b = 10$  cm) were placed around the detector-housing (length: 11.6 cm; diameter: 8 cm), which includes the germanium-crystal. Subsequently, plates without perforation followed. The total length  $a$  of all plates varied for different samples.

**Table 2**

Characteristics of the detectors, DARIO (D) at MPI-K (Heidelberg, Germany) and GeMPI (G) at LNGS (Assergi, Italy) [3], used for screening of the stainless steel samples

Detector	DARIO	GeMPI
Type	HP coax p-type	HP coax p-type
Crystal size ( $\varnothing \times l$ ) (mm <sup>2</sup> )	59.7 × 61	77.5 × 88.5
Active mass (kg)	0.83	2.2
Relative efficiency (%)	31	102
FHWM @ 1332 keV (keV)	2.6	2.3
Sample chamber (l)	11.0	15.0
Sensitivity	<sup>226</sup> Ra: 0.6 mBq/kg <sup>228</sup> Th: 0.5 mBq/kg <sup>40</sup> K: 1.7 mBq/kg	<sup>226</sup> Ra: 16 μBq/kg <sup>228</sup> Th: 19 μBq/kg <sup>40</sup> K: 88 μBq/kg

progenies on the stainless steel samples, the measurements started only 1–3 days after the sample insertion in the sample chambers. The measurement time varied between 3.0 and 19.6 d.

### 3. Process of evaluation

#### 3.1. Efficiency determination via Monte Carlo simulations

Monte Carlo simulations for the calculation of the full-energy peak efficiencies of the detectors were performed at MPI-K (using the simulation tool MaGe [10] based on Geant 4.8.2) and at LNGS (using Geant 3.21).

For the estimation of the uncertainties in the evaluation and to test the compatibility of the results, both laboratories at MPI-K and LNGS performed calibration measurements and participated in different radioactivity comparison studies. The comparison of the MC simulated results with radioactivity standards allowed an estimation of the systematic uncertainties. For DARIO, a relative deviation from expected value of up to max. 20% was found [11], while the accuracy for the GeMPI detector was estimated to be 5%. These two values are taken into account in the uncertainty budget of the results in Table 3.

Moreover, a sample has been measured by both detectors (measurements D2 and G6; for the notation see Section 4). The

rather good agreement between the finite values<sup>2</sup> estimated with both detectors, provides confidence in the simulated values also in the present case of large samples with high density.

#### 3.2. Calculation of the radioactivity concentrations

The radioisotope concentrations in the stainless steel samples were estimated from the intensities of the appropriate  $\gamma$ -lines in the energy spectrum assuming homogeneous distribution in the bulk material.

The single lines were evaluated according to the DIN standard 25482-5 [12]. In the case of decay chains or radionuclides with more than one line, the obtained single line results were combined to a weighted average or a combined upper limit. A more detailed description of the whole procedure can be found in Ref. [13]. For finite results a coverage factor  $k = 1$  (68% confidence level CL) was chosen, while a 90% C.L. was chosen to report the upper limits.

Concluding, the selection of lines is illustrated here by means of the primordial radionuclides: for <sup>40</sup>K the 1460.8 keV-line was used. Within the <sup>232</sup>Th decay chain the dominant lines at 238.6 keV, 583.2 keV, 2614.5 keV denote the <sup>228</sup>Th subchain and the 911 keV-line that of <sup>228</sup>Ra. Regarding the <sup>238</sup>U decay chain 186 keV, 295.2 keV, 352.9 keV, 609.4 keV, 1120.4 keV, 1764.6 keV were selected for <sup>226</sup>Ra and their progenies. The weak 1001 keV-line was used for <sup>234m</sup>Pa. This radioisotope is separated from <sup>238</sup>U only by the shortlived <sup>234</sup>Th and thus represents the concentration of its parent.

A more subtle treatment is required for the estimation of <sup>235</sup>U: its concentration is evaluated from the 186 keV-line, which overlaps with the <sup>226</sup>Ra-line at the same energy. Thus, the <sup>226</sup>Ra concentration is firstly evaluated from the remaining <sup>226</sup>Ra-lines listed above. From here, the contribution from <sup>226</sup>Ra in the 186 keV-line is estimated and subtracted from the total peak. The remaining excess counts in the line peak belongs to <sup>235</sup>U.

### 4. Discussion of the results

The results of the radioisotope concentrations in the different samples are summarized in Table 3.

The nomenclature D1–D7 and G1–G7 arises from the detector names DARIO (D) and GeMPI (G), the numbers from the chronological order of the measurements.

The batches of stainless steel were produced by the following manufacturers: Industeel, Germany (D1), Ilsenburg, Germany (D2–D7; G1–G2, G6), Ugine & Alz, Belgium (G3) and Acroni, Slovenia (G4–G5, G7).

#### 4.1. Primordial radionuclides

Table 3 shows that the U- and Th-concentrations are low compared to the values of (5–17) mBq/kg <sup>226</sup>Ra and (5–12) mBq/kg <sup>228</sup>Th in the stainless steel samples reported in Ref. [5].

Regarding the <sup>228</sup>Th concentrations, which are of major relevance for GERDA, all investigated samples are below the aimed level of 10 mBq/kg. Many of them are below 2 mBq/kg <sup>228</sup>Th and D6, D7, G1, G2, G3, G6 even have an upper limit < 1 mBq/kg <sup>228</sup>Th. To our knowledge, G2 shows the lowest <sup>228</sup>Th limit ever measured for stainless steel.

The surprising discovery of such low concentrations of <sup>228</sup>Th led to the replacement of batches with approx. 5 mBq/kg <sup>228</sup>Th

<sup>2</sup> I.e. for <sup>60</sup>Co and <sup>7</sup>Be; the <sup>7</sup>Be-activity decreased as expected between the first (D2) and second (G6) measurement; see Section 4.3.1.

**Table 3**

Part 1: concentrations of primordial, anthropogenic and cosmogenic radionuclides given in (mBq/kg) for the 1.4571 stainless steel measured with the detectors DARIO (D) at MPI-K (Heidelberg, Germany) and GeMPI (G) at LNGS (Gran Sasso, Italy)

Sample	D1	D2	D3	D4	D5	D6	D7
Exposure	158.5	243.2	384.8	443.6	241.8	521.3	217.56
Vendor	IS	IB	IB	IB	IB	IB	IB
<sup>228</sup> Ra	<3.0	<3.5	<3.6	<3.8	<1.8	<1.4	<4.2
<sup>228</sup> Th	3.4 ± 1.0	<1.7	<1.9	<1.8	<1.1	<0.8	<1.0
<sup>226</sup> Ra	<2.6	<2.0	<0.9	<1.6	<1.5	<0.6	<1.4
<sup>234m</sup> Pa	<155	<100	<84	<53	<76	<38	<152
<sup>40</sup> K	<4.0	<4.7	<3.4	<3.3	<3.2	<1.8	<7.2
<sup>60</sup> Co	6.6 ± 1.1	14.4 ± 2.1	15.4 ± 2.2	14.8 ± 2.1	16.8 ± 2.5	16.8 ± 2.4	17.5 ± 2.6
<sup>7</sup> Be		34.6 ± 5.3					
Sample	G1	G2	G3	G4	G5	G6	G7
Exposure	174.9	1072.4	178.9	195.6	510.1	294.1	331.3
Vendor	IB	IB	U	A	A	IB	A
<sup>228</sup> Ra	<2.6	<0.86	<1.0	<3.0	1.0 ± 0.5	<1.1	1.9 ± 1.0
<sup>228</sup> Th	<0.20	<0.11	<0.41	5.1 ± 0.5	1.5 ± 0.2	<0.27	5.2 ± 0.5
<sup>226</sup> Ra	<1.3	<0.24	<0.74	<1.3	1.0 ± 0.6	<0.35	3.9 ± 1.6
<sup>234m</sup> Pa	<94	<12	<45	<41	54 ± 16	<38	<56
<sup>235</sup> U	<2.6	<0.63	<1.5	<1.9	2.5 ± 1.5	<1.5	<3.9
<sup>40</sup> K	<2.8	<0.93	<1.1	<1.7	<0.81	<1.1	<1.7
<sup>60</sup> Co	45.5 ± 2.1	14.0 ± 0.1	13.8 ± 0.7	20 ± 1	18.3 ± 0.7	13 ± 0.6	42.1 ± 1.9
<sup>137</sup> Cs	0.77 ± 0.43	<0.16	<0.26	<0.36	<0.1	<0.39	<0.6
<sup>7</sup> Be	<3.9	<3.0	<5.7	9.6 ± 2.9	4.8 ± 1.7	13.6 ± 2.5	<5.9
<sup>54</sup> Mn	1.3 ± 0.4	1.5 ± 0.1	0.92 ± 0.24	2.0 ± 0.3	1.7 ± 0.2	1.4 ± 0.2	1.6 ± 0.3
<sup>58</sup> Co	0.67 ± 0.34	0.99 ± 0.12	0.56 ± 0.23	0.71 ± 0.26	0.69 ± 0.16	0.59 ± 0.20	0.54 ± 0.27
<sup>56</sup> Co	<0.32	0.17 ± 0.06	<0.62	<0.71	0.28 ± 0.10	<0.42	<0.6
<sup>46</sup> Sc	<0.35	0.24 ± 0.06	<0.54	<0.67	0.47 ± 0.14	<0.31	0.61 ± 0.26
<sup>48</sup> V	0.30 ± 0.11	0.36 ± 0.07	0.27 ± 0.11	0.31 ± 0.13	0.22 ± 0.09	0.40 ± 0.12	0.39 ± 0.13

Row 2 corresponds to the exposure, which is given in (kg d). As expected, a higher exposure leads tendentially to a higher sensitivity. Row 3 contains the abbreviations of the manufacturers: IS (Industeel), IB (Ilsenburg), U (Ugine & Alz) and A (Acroni). The numbers shows that the obtained concentrations and eventual deviations from secular equilibrium in the natural decay chains are related to the differences of the melting techniques adapted by the manufacturers.

(i.e. G4 and G7), so that all accepted batches have a concentration below 2 mBq/kg <sup>228</sup>Th except one batch (D1), which has still (3.4 ± 1.0) mBq/kg <sup>228</sup>Th.

For <sup>226</sup>Ra, concentrations <4.2 mBq/kg were found.

The <sup>235</sup>U-concentration, established only for the G1–G7 measurements, is also <3.9 mBq/kg.

Finally, in the case of <sup>40</sup>K, only upper limits <7.2 mBq/kg could be determined for the GERDA samples.

#### 4.1.1. Representativeness of the measurements

During the measurement campaign, 575 kg of stainless steel from 13 different batches was screened. Since ca. 25 tons deriving from these batches are used for building the GERDA cryostat, it is justified to inquire the representativeness of the screened samples.

A first problem could be related to an inhomogeneous distribution of elements in the melt. An exceeding temperature-stratification could e.g. confine convective processes [14]. As strict chemistry specifications are demanded to allow ideal mechanical properties, a relatively high homogeneity is expected. The samples G2 and G6, which belong to different batches of a single melt, allow a direct test. The similar <sup>60</sup>Co concentrations contained in both samples confirm the above hypothesis. On the other hand the observed <sup>7</sup>Be-concentrations disagree. However, since <sup>7</sup>Be is contained in atmospheric dust (see Section 4.3.1), it may be introduced accidentally before each measurement. Thus, it is not a good indicator for homogeneous distributions in bulk material.

A second problem could be the presence of local hot spots in marginal regions of the melt. During the melting process, a clear

separation into melt, slag lying on the melt surface and escaping dust is usually observed (so-called ‘fractioning’). From experiments concerning refining processes in stainless steel, Warren and Clark (1995) [14] concluded, that highly reactive elements, including transuranics (lanthanides, actinides and other fission products), oxidize from ferrous metals. However, transition elements such as cobalt (see Section 4.2) or technetium are poorly removed from the melt. Indeed, several authors [14–16] found, that the concentration of U and Th remaining in the melt and dust is <5% and those in the slag is between (95–100)%. That means, that the effectiveness of removing the entire slag and other impurities in the melt of stainless steel could be of major importance.

#### 4.1.2. Deviations from secular equilibrium in the <sup>238</sup>U and <sup>232</sup>Th decay chains

In this section, deviations from secular equilibrium in the decay chains of U and Th are discussed, by means of the three GERDA samples G4, G5 and G7.

Regarding the <sup>238</sup>U decay chain, a clear deviation from secular equilibrium is observed for the ratio of the progenies <sup>234m</sup>Pa and <sup>226</sup>Ra in G5. <sup>226</sup>Ra results to have a 50 to 60 times lower concentration than <sup>234m</sup>Pa and <sup>238</sup>U, respectively.

Regarding the <sup>232</sup>Th decay chain, G5 shows a rather good secular equilibrium between <sup>228</sup>Ra and <sup>228</sup>Th. However, this is not the case for G4 and G7. As Fig. 3 shows, the presence of a non-equilibrium in the <sup>232</sup>Th decay chain (after removal of <sup>228</sup>Ra) could lead to a notable increase of the <sup>228</sup>Th-activity within a time frame of 1–2 decades. For most of the GERDA samples, only upper limits



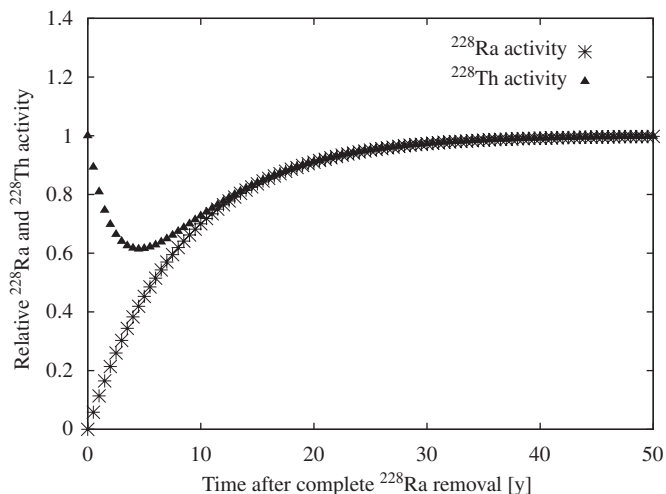


**Fig. 3.** Deviation from secular equilibrium in the Th decay chain: herein,  $^{228}\text{Ra}$  is completely absent at time  $t = 0$  and the  $^{228}\text{Th}$ -concentration is normalized to 1. The curves of the changing  $^{228}\text{Ra}$ - and  $^{228}\text{Th}$ -concentrations over time  $t$  are illustrated.

could be estimated, which do not allow to exclude the scenario of deviation from secular equilibrium in the Th decay chain.

Looking at the melting technique typically used (i.e. electric arc furnace), deviations from secular equilibrium within the decay chains are introduced rather through additives in the iron–steel conversion [17,18] than through the fractioning process as described in Section 4.1.1.

## 4.2. Anthropogenic radionuclides

### 4.2.1. $^{60}\text{Co}$

The major contaminant detected in the GERDA stainless steel samples is  $^{60}\text{Co}$  ( $\tau_{1/2} = 5.27$  y). It is one of the most common artificial radionuclides, but it can also be produced via cosmic activation.

Radioactive materials were introduced originally in the refractory lining of blast furnace to monitor the lining thickness and abrasion of these sealed vessels. This contributed to an increase of the  $^{60}\text{Co}$  concentration in steel produced over the last decades [14].

Further,  $^{60}\text{Co}$  and other radionuclides have been introduced through recycled scrap, the main raw material for stainless steel production, by controlled release of radioactive metals (e.g. from nuclear plants or pipes/large vessels from oil-industry) or inadvertent/accidental melting of ‘orphan sources’ (e.g. not properly disposed medical sources) [16].

The measured concentration levels are in the range of (6.6–45.5) mBq/kg with a mean value of 19 mBq/kg (13 batches). This is similar to 13 mBq/kg found in previous measurements of steel (10 batches) by Köhler et al. [19].

For GERDA, the rather high  $^{60}\text{Co}$ -concentration (compared with the primordial radionuclides) in the stainless steel vessels of the cryostat is tolerable: as simulations showed [20,21], the 1173- and 1333 keV- $\gamma$ -quanta will cause a negligible contribution to the background in GERDA due to the copper shielding and the LAr. Also the contribution of the 2506 keV- $\gamma$ -quanta (branching ratio:  $2 \times 10^{-8}$ ) will be non-critical (in comparison with the simulated background from the 2615 keV-line [4]).

### 4.2.2. $^{137}\text{Cs}$

Regarding the other manmade radionuclides, only the concentration of  $^{137}\text{Cs}$  for the measurements G1–G7 was estimated.

With the exception of G1, which had a concentration of  $(0.77 \pm 0.43)$  mBq/kg, only upper limits below  $<0.6$  mBq/kg could be found.

## 4.3. Cosmogenic radionuclides

### 4.3.1. $^7\text{Be}$

Among the cosmogenic radionuclides,  $^7\text{Be}$  ( $\tau_{1/2} = 53.2$  d) showed the highest concentration. This was especially the case for the sample in measurement D2 at MPI-K. The concentration was  $(34.6 \pm 5.3)$  mBq/kg. Sixty-three days later a subsequent measurement (G6) at LNGS of the same sample was found to be  $(13.6 \pm 2.5)$  mBq/kg. Considering the decay time, this second estimation confirmed well the previous one and demonstrated also the compatibility of the efficiencies simulated by both laboratories (see Section 3.1).

The appearance of  $^7\text{Be}$  in stainless steel is quite surprising.  $^7\text{Be}$  is produced through spallation of N and O in the stratosphere and upper troposphere [22]. Its average production rate is about 3 mBq/m<sup>3</sup> and the ash of collected dust from the atmosphere (by which the atmospheric activity is determined) has a mean activity of 400 kBq/kg. Seasonal and local variation can be expected [23,24]. The dust/ash ratio is not well known, but might be in the range of 10. The deposition of such dust via processes in the melt or on surfaces not yet identified could partially explain the observed contamination.

On the other hand, a direct cosmic ray production of  $^7\text{Be}$  by spallation in ferrous materials has a relatively low probability.

### 4.3.2. Others

Regarding the other cosmogenic isotopes,  $^{56}\text{Co}$ ,  $^{58}\text{Co}$ ,  $^{54}\text{Mn}$ ,  $^{48}\text{V}$  and  $^{46}\text{Sc}$  were detected. They are produced, respectively, by the stable isotopes  $^{58}\text{Ni}$ ,  $^{60}\text{Ni}$ ,  $^{56}\text{Fe}$ ,  $^{50}\text{Cr}$  and  $^{48}\text{Ti}$  via neutron induced spallation reactions. An alternative production channel, but to a lower extent, is the negative muon capture reaction ( $\mu^-$ ,  $\nu 2n$ ) [25].

The production rates for the relevant reactions are only known for  $^{58}\text{Co}$  and  $^{54}\text{Mn}$ , namely 0.4 mBq/kg [26] and 4.5 mBq/kg [9] per week, at a shielding depth of 2 m w.e. and at sea level, respectively. Future measurements are planned to obtain further information on the production rates for 1.4571 stainless steel via the exposure of one GERDA sample at sea level with a subsequent analysis.

The concentrations of the cosmogenic isotopes in the GERDA samples are generally in the range of 1 mBq/kg and below. Therefore they do not present a problem for the experiment.

## 5. Conclusions

The radioisotope concentrations in 1.4571 (DIN EN 10088) stainless steel for the GERDA experiment have been determined. The measurements showed for the first time the availability of batches with very low concentrations in the range of 1 mBq/kg and below for the primordial and cosmogenic radionuclides. These concentrations are at least one order of magnitude lower than those obtained for stainless steel in the Borexino experiment. As a consequence, this discovery allowed a significant reduction of the amount of costly ultrapure copper used as inner shielding in the GERDA experiment.

The possibility of deviation from secular equilibrium in the primordial decay chains has been discussed. Indeed, deviations in the Th decay chain for two samples and in the U decay chain for a single sample were observed. Mass spectrometry (ICP-MS), which is also used for the estimation of trace elements in materials, is not able to prove such deviations, because it measures only the long-lived mother nuclides  $^{232}\text{Th}$  and  $^{238}\text{U}$ . In contrast,  $\gamma$ -ray

spectrometry has this ability detecting the  $\gamma$ -quanta from the short-lived progenies in the subchain of the U and Th decay chains. Taking into account that the most dangerous  $\gamma$ -emitters within the U and Th decay chains are usually in the later subchain,  $\gamma$ -ray spectrometry results to be the most direct screening technique. This demonstrates its unique role for rare-event experiments like GERDA, in which a high radiopurity of the used materials is required.

### Acknowledgments

We sincerely thank the company NIRONIT Edelstahlhandel GmbH & Co.KA for its cooperation and the mechanical workshop at MPI-K for its support throughout the stainless steel measurement campaign. We would like to acknowledge the support by INTAS (Project Nr. 05-1000008-7996) and by DFG within the SFB Transregio 27 'Neutrinos and Beyond'.

### References

- [1] I. Abt, et al. (GERDA Collaboration), Proposal to LNGS P38/04, 2004.
- [2] I. Bergström, et al., Phys. Rev. Lett. 86 (19) (2001) 4259.
- [3] G. Heusser, et al., in: P.P. Povinec, J.A. Sanchez-Cabeza (Eds.), Radionuclides in the Environment, Elsevier, Amsterdam, 2006, pp. 495–510.
- [4] I. Barabanov, et al., Nucl. Instr. and Meth. A, 2008, to appear.
- [5] C. Arpesella, BOREXINO Collaboration, et al., Astropart. Phys. 18 (2002) 1.
- [6] DIN EN 10088-1:2005-09, Nichtrostende Stähle - Teil 1: Verzeichnis der nichtrostenden Stähle, German edition EN 10088-1:2005, Beuth Verlag GmbH, 2005.
- [7] G. Heusser, Nucl. Instr. and Meth. B 58 (1991) 79.
- [8] H. Neder, et al., Appl. Radiat. Isot. 53 (2000) 191.
- [9] G. Heusser, in: M. Garcia-Leon, R. Garcia-Tenorio, (Eds.), Proceedings of the 3rd International Summer School, Huelva, 1993, World Scientific, Singapore, 1994, pp. 69–112.
- [10] Y.D. Chan, et al., IEEE Trans. Nucl. Sci. 2008, submitted.
- [11] D. Budjäs, et al., AIP Conf. Proc. 897 (2007) 26.
- [12] DIN 25482-5, Nachweisgrenze und Erkennungsgrenze bei Kernstrahlungsmessungen - Zählende hochaufgelöste gammaspektrometrische Messungen ohne Berücksichtigung des Probenbeeinflussungseinflusses, German edition, Beuth Verlag GmbH, 1993.
- [13] W. Maneschg, Diploma Thesis, University of Heidelberg, 2007.
- [14] NCRP Report No. 141, Section 6.3, National Council on Radiation Protection and Measurements, Bethesda, Maryland, 2002.
- [15] U. Quade, IECM'01, The 8th International Conference on Radioactive Waste Management and Environmental Remediation, September 30–October 4, 2001, Bruges, Belgium, 2001, pp. 1–4.
- [16] D. Neuschütz, et al., ISJ Int. 45(2) (2005) 288.
- [17] D. Neuschütz, private communication, 2007.
- [18] E. Pernicka, private communication, 2007.
- [19] M. Köhler, et al., Appl. Radiat. Isot. 61 (2004) 207.
- [20] G. Bonvini, Diploma Thesis, University of Heidelberg, 2007.
- [21] L. Pandola, private communication, 2007.
- [22] D. Lal, B. Peters, Cosmic ray produced radioactivity on Earth, in: L.K. Sitte (Ed.), Handbuch der Physik, vol. 46(2), Springer, New York, 1967, pp. 551–612.
- [23] H. Wershofen, PTB Braunschweig (Germany), private communication, 2007.
- [24] M. Yamamoto, et al., J. Environ. Radiat. 86 (2006) 110.
- [25] G. Heusser, Nucl. Instr. and Meth. A 369 (1996) 539.
- [26] W. Hampel, Ph.D. Thesis, University of Heidelberg, 1974.